A new cropland area database by country circa 2020

Francesco N. Tubiello[1*], Giulia Conchedda[1], Leon Casse[1], Pengyu Hao[2], Giorgia de Santis[1] and Zhongxin Chen[2]

[1]Statistics Division, Food and Agriculture Organization of the United Nations, Viale delle Terme di Caracalla, Rome, Italy.
[2]Digitalization and Informatics Division, Food and Agriculture Organization of the United Nations, Viale delle Terme di Caracalla, Rome, Italy.

*Corresponding author: francesco.tubiello@fao.org

Abstract

We describe a new dataset of cropland area circa the year 2020, with global coverage, with data for 221 countries and territories and 34 regional aggregates. Data are generated from geospatial information on the agreement-disagreement characteristics of six open access high-resolution cropland maps derived from remote sensing. The cropland area mapping (CAM) aggregation dataset provides information on: i) mean cropland area and its uncertainty; ii) cropland area by six distinct cropland agreement classes; and iii) cropland area by specific combinations of underlying land cover product. The results indicated that world cropland area is 1500 ± 400 million hectares (Mha) (mean and 95% confidence interval), with a relative uncertainty of 25% that increased across regions. It was 50% in Central Asia (40 ± 20 Mha), South America (180 ± 80 Mha), and Southern Europe (40 ± 20 Mha); up to 40% in Australia and New Zealand (50 ± 20 Mha), South-eastern Asia (80 ± 30 Mha) and Southern Africa (16 ± 6 Mha). Conversely, cropland area was estimated with better precision, i.e. smaller uncertainties in the range 10%-25% in Southern Asia (230 ± 30 Mha), Northern America (200 ± 40 Mha), Northern Africa (40 ± 10 Mha), and Eastern and Western Europe (40 ± 10 Mha). The new data can be used to investigate coherence of information across the six underlying products, as well as to explore important disagreement features. Overall, 70% or more of the estimated mean cropland area globally and by region corresponded to good agreement of underlying land cover maps — four or more. Conversely, in Africa cropland area estimates found significant disagreement, highlighting mapping difficulties in complex landscapes. Finally, the new cropland area data were consistent with FAOSTAT in 15 out of 18 world regions, and for 114 out of 182 countries with a cropland area above 10 kha. By helping to highlight features of cropland characteristics and underlying causes for agreement/disagreement across land cover products, the CAM aggregation dataset may be used as a reference for the quality of country statistics and may help guiding future mapping efforts towards improved agricultural monitoring. Data are publicly available at: https://doi.org/10.5281/zenodo.7987515 (Tubiello et al., 2023a).

1 Introduction

Information on cropland area is needed to assess and monitor the sustainability of agriculture at local, regional and planetary scales. Information on world cropland area with national or sub-national detail is currently available as: i) Statistics of agricultural land use, collected from countries by the Food and Agriculture Organizations of the United Nations (FAO) and disseminated in FAOSTAT (FAO, 2023a); and ii) land cover maps produced from remote sensing (Potapov et al., 2022a). These historically rather distinct sources are becoming interconnected, with remote sensed data increasingly complementing more traditional data sources such as agricultural censuses and surveys (Miller et al., 2009; Bailey and Boryan, 2010; FAO, 2018; Karthikeyan et al., 2020; Weiss et al., 2020; Bey et al., 2016). Comparison analyses at multiple scales of these different sources have been published to facilitate in-depth understanding of cropland characteristics and to derive methods for data selection and applications (Bratic et al, 2019; Liu et al., 2021; Venter et al., 2022; Chaaban et al., 2022; Ding et al., 2022). We recently conducted a meta-analysis of the currently available six independent high resolution (10–30 m) land cover maps circa 2020 and derived a map on cropland agreement/disagreement at pixel level — the CAM map — showing that by combining such information world cropland area can be estimated to within 25% of the mean cropland area (Tubiello et al., 2023b). That study identified 'definitional bias,' i.e., systematic errors due to imperfectly aligned land cover/land use definitions, as an important source of uncertainty in addition to well-described factors such as differences in data sources, pre-processing methods and validation approaches (Fritz et al., 2013; Gao et al., 2020, Wang et al., 2019). The cropland agreement map is already being used in support of relevant geospatial work (e.g., Tang et al., 2023).

This study presents a new database of cropland area at country level, based on the geospatial work of Tubiello et al. (2023b). We aggregated pixel level information and quantified means and uncertainties of cropland area at country and regional level. The new database, referred to hereafter as Cropland Agreement Mapping (CAM) aggregation dataset, provides information on cropland area by country, with data on: i) mean estimate and uncertainty; ii) contributions to total area by agreement class; iii) contributions to total area by specific combinations of the underlying land cover products. This novel information helps to understand better the linkage between agricultural land cover and land use information and related uncertainty, offering useful insights with regards to future mapping efforts and their evaluation. The CAM dataset is available as open access data at: https://doi.org/10.5281/zenodo.7987515 (Tubiello et al., 2023a).

2 Materials and Methods

2.1 Cropland agreement map

We used the CAM map by Tubiello et al. (2023b) as input to generate country statistics. The CAM map
70 consolidates information from six high-resolution land cover maps based on a meta-analysis done within
the code editor of the Google Earth Engine (GEE) (Gorelick et al., 2017). These six maps are: ESRI (Karra
et al. 2021); FROM_GLC Plus (Yu et al., 2022); GLAD (Potapov et al, 2022a); GLC-FCS30-2020 (Zhang
et al., 2021); Globeland30 (Chen et al., 2015); and WorldCover (Zanaga et al., 2021). Appendix A further
provides details on the characteristics of the six land cover maps, along with their spatial consistency and
75 similarity analysis.

The CAM actually consists of two geospatial layers prepared at 30 m resolution as 8-bit unsigned integers
using WGS84 (EPSG:4326) coordinate system: i) a *simple cropland agreement* map; and ii) a *detailed
cropland agreement* map.

The *simple cropland agreement* map layer combines six cropland binary masks (with values of 1 for
80 cropland, 0 for no cropland) from the six input land cover products (Appendix A), into a map with pixel
values ranging 1-–6, representing, when normalised by the number of layers, the probability of cropland
area in each pixel.

The *detailed cropland agreement map* layer contains information on the individual land cover products and
their combinations, with values ranging between 0 (bit 00000000, corresponding to no cropland), and 63
85 (bit 00111111, representing complete agreement) (Appendix B, Tab. B1). Each input dataset contains
omission and commission errors, which affect their accuracy (Tab. 1). While the uncertainty information
in CAM and in our dataset is computed net of these accuracies, it should be noted that synergic
combinations of multiple land cover products typically yield improved accuracies (Lu et al., 2020) as
overall omissions and commissions errors may be reduced.

90 As discussed elsewhere (Tubiello et al., 2023b), the definitions of 'cropland' as a land cover class varied
across the six products (Tab. 1), although they largely corresponded to FAO land use class *cropland* or
arable land (Tab. 2). Specifically, of the six products used as input, GLAD, WorldCover and ESRI
'cropland' classes could conceptually be mapped to FAO land use class *arable land* or *temporary crops*,
while the other three maps, including information on shrubs and woody components, could be better aligned
95 with the FAO parent class *cropland* (Tubiello et al., 2023b). Within the latter, Globeland30 included within
'cropland' tree and shrub crops directly under a single class (cultivated land); FROM-GLC included
permanent shrubs crops while excluding tree crops; and FCS30 provided data on cropland globally, with

some partial regional distinctions between herbaceous and woody crops within irrigated/rainfed sub-classes (Tab. 1). The latter category was excluded to reduce definitional bias in the consolidated product.

100 **Table 1.** Cropland definitions and accuracy of the six input layers used for the cropland agreement map.

Dataset	Label	Definition	Cropland class #	Accuracy[a]
ESRI (ESR)	Crops	Human planted/plotted cereals, grasses, and crops not at tree height; examples: corn, wheat, soy, fallow plots of structured land.	5	PA 89.9%; UA 91%
FROM-GLC Plus[b] (FRG)	Croplands	Land that has clear traits of intensive human activity. It varies a lot from bare field, seeding, crop growing to harvesting. It includes arable and tillage land with herbaceous/shrub crops and land with plastic foam or grass roof protection with distinguishing spectral properties. Fruit trees are classified into forests.	10 – Level 1	OA 71.9%
GLAD (GLD)	Cropland	Land used for annual and perennial herbaceous crops for human consumption, forage (including hay) and biofuel. Perennial woody crops, permanent pastures and shifting cultivation are excluded from the definition. The fallow length is limited to 4 years for the cropland class.	1	PA 86.4%; UA: 88.5%
GLC-FCS30-2020[c] (FCS30)	Cropland	Rainfed cropland, Irrigated cropland Herbaceous cover Tree or shrub cover (Orchard)	10 – Level 1 20 – Level 1 11 – Level 2 12 – Level 2[d]	PA 88.0%; UA 83.9%
Globeland30 (GL30)	Cultivated land	Category includes paddy fields, irrigated dry land, rain-fed dry land, vegetable land, pasture planting land, greenhouse land, land mainly for planting crops with fruit trees and other economic trees, as well as tea gardens, coffee gardens and other shrubs.	10	OA 85.7%
WorldCover (WCO)	Cropland	Land covered with annual cropland that is sowed/planted and harvestable at least once within the 12 months after the sowing/planting date. The annual cropland produces an herbaceous cover and is sometimes combined with some tree or woody vegetation. Note that perennial woody crops will be classified as the appropriate tree cover or shrub land cover type. Greenhouses are considered as built-up.	40	PA 76.7%; UA 81.1%

[a] When available, user and producer accuracy (UA and PA) of the cropland class, overall map accuracy (OA) is otherwise reported. [b] Accuracy results reported for the 2020 map from the data producers (personal communication). [c] Accuracy results based on the 2015 version of the map. [d] Excluded from the cropland agreement map.

105

110

2.2 Preparation of the CAM aggregation dataset

The country statistics populating the CAM aggregation dataset (Tubiello et al., 2023a) were extracted from
the simple and detailed agreement maps discussed above (Tubiello et al., 2023b), using the FAO Global
Administrative Unit layer (GAUL) for country boundaries (FAO 2015) — also accessible from the GEE
Code editor. The cloud processing method in GEE generates country area statistics inherently taking into
account the different pixel areas by latitude. The aggregation to country level was done by summing these
pixels (i.e. pixel counting) for the simple or detailed classes of agreement as well as for the 6 cropland
layers in the CAM aggregation dataset.

Generally, for n land cover maps, pixel values in the *simple agreement map* belong to a set of $n+1$ elements,
$\{0, 1/n, 2/n, (n-1)/n, 1\}$, representing the level of agreement among input maps, which was interpreted as
the probability of finding cropland in each pixel by Tubiello et al. (2023b). By aggregating the pixel-level
information at national scale it was therefore possible to generate country estimates of: i) mean cropland
area A and associated uncertainty: ii) cropland area by agreement class, SA_1 to SA_6, with SA_k representing
the area where k maps agreed, and $A = \Sigma_k SA_k$ (Fig. 1); and iii) cropland area by specific map combinations.

Following the steps above, we generated values for over 221 countries and 34 territories, with country codes
aligned to standard M49 area codes classification.

In terms of simple agreement classes, SA_1 represents the contribution to cropland area by single land cover
products, while SA_6 provides information on the contribution to cropland area when all six products agree.
Similarly, for each agreement class SA_k, data represent the contributions to total cropland area by all
relevant combinations of k products. With respect to the two extreme cases, definitional bias would be small
for SA_6, with the CAM map likely estimating the subcomponent *temporary crops* rather than *cropland*,
since the former category would be the only one that could be detected by all land cover products. By the
same token, definitional bias would be higher for SA_k classes with lower k values and highest for SA_1, with
CAM including in such cases more subcomponents of cropland that would not be equally detected by the
underlying land cover products, for instance *temporary meadows and pastures* or *permanent crops*. To this
end, the CAM data on detailed cropland agreement provide additional information on which specific
combinations of k land cover products contributed to class SA_k in a given country. For example, the area of
SA_3 in country i could be the sum of agreement areas identified by GLAD-WorldCover-ESRI and GLAD-
WorldCover-FROM_GLC.

Figure 1. Simple cropland agreement map. Adapted from Tubiello et al. (2023b).
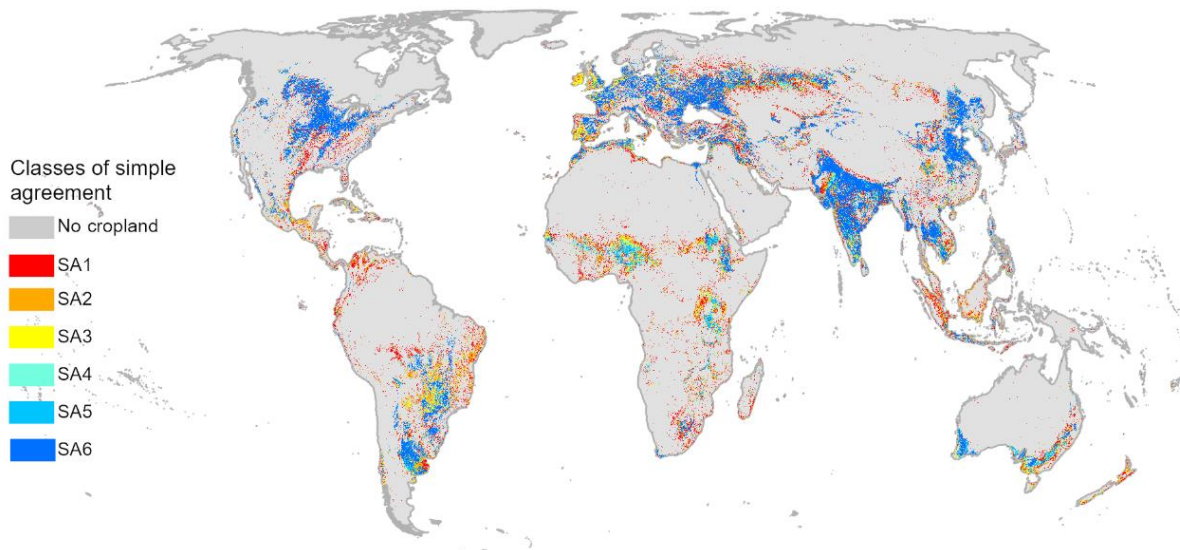
145

2.3 Comparison with FAO land use statistics

FAO land use statistics of cropland and arable land are routinely used as benchmark to assess the robustness of land cover information at various scales (Vancutsem et al., 2013; Yu et al., 2014; Pérez-Hoyos et al.,

150   2017; Xu et al., 2019; Li and Xu., 2020; Potapov et al., 2022a). We compared the cropland area estimates of the CAM aggregation dataset against FAOSTAT (FAO, 2023a) area statistics of *cropland* (Tab. 2), quantifying goodness of fit in terms of the coefficient of determination (R^2) and a normalized root-mean square error (NRMSE, expressed in % and computed by dividing RMSE by the range of values). Possibly due to variations in land and water masks, many small island states were absent in one or more of the six

155   land cover inputs used in CAM. To ensure consistency, a minimum cut-off value of 10 thousand hectares (kha) of cropland was applied, resulting in 182 complete country records in CAM, out of the total 221 countries covered.

160

Table 2. FAO land use categories for cropland as defined in the FAO Land Use, Irrigation and Agricultural Practices questionnaire (FAO, 2023a).

Land use category	Definition
Cropland	Land used for cultivation of crops. The total of areas under *Arable land* and *Permanent crops*.
Arable land	Land used for cultivation of crops in rotation with fallow, meadows and pastures within cycles of up to five years. The total of areas under *Temporary crops*; *Temporary meadows and pastures*; and *Temporary fallow*. *Arable land* does not include land that is potentially cultivable but is not cultivated.
Temporary crops	Land used for crops with a less-than-one-year growing cycle, which must be newly sown or planted for further production after the harvest. Some crops that remain in the field for more than one year may also be considered as temporary crops e.g., asparagus, strawberries, pineapples, bananas and sugar cane. Multiple-cropped areas are counted only once.
Temporary fallow	Land that is not seeded for one or more growing seasons. The maximum idle period is usually less than five years. This land may be in the form sown for the exclusive production of green manure. Land remaining fallow for too long may acquire characteristics requiring it to be reclassified, as for instance *Permanent meadows and pastures*, if used for grazing or haying.
Temporary meadows and pastures	Land temporarily cultivated with herbaceous forage crops for mowing or pasture, as part of crop rotation periods of less than five years.
Permanent crops	Land cultivated with long-term crops which do not have to be replanted for several years (such as cocoa and coffee), land under trees and shrubs producing flowers (such as roses and jasmine), and nurseries (except those for forest trees, which should be classified under "Forestry"). Permanent meadows and pastures are excluded from permanent crops.

2.4 Uncertainty and use of significant figures

165   The data made available through the CAM aggregation dataset are area estimates based on samples of size *n*=6 (one value per land cover map). Cropland area was thus estimated as: $A = x \pm u$, with *x* being the sample mean and *u* its uncertainty, defined herein as a 95% confidence interval and computed as the estimated standard error of the mean multiplied by 2.57—the corresponding value of the two-tailed t-Student distribution for *n*-1 = 5 degrees of freedom. We reported results using only one significant figure

170   for the uncertainty, following recommendations of the International Bureau of Weights and Measures (BIPM) for small sample sizes (JCGM, 2009).

3 Results and discussion

3.1 Cropland area

175   **3.1.1 Global and regional results**

CAM aggregated data indicated a total world cropland area in year 2020 of 1500 ± 400 million hectares (Mha), with a relative uncertainty of 27%. Uncertainty was higher across regions—up to 50% for Africa,

Americas, Asia, Europe and 40% for Oceania (Tab. 3). The world's cropland area was very close to, and statistically consistent with the corresponding FAOSTAT value (1560 Mha). Comparisons of regional cropland area were also largely consistent with FAOSTAT, with $R^2 = 0.92$ and NRMSE of 8% (Fig. 2). With reference to Tab. 3, of the 18 world sub-regions considered, only three cropland area estimates were statistically inconsistent with FAOSTAT, namely Middle Africa, where we computed 16 ± 7 Mha vs. 37 Mha in FAOSTAT; Western Africa, 60 ± 20 Mha vs. 102 Mha in FAOSTAT; and South-eastern Asia, 80 ± 30 M ha vs. 123 M ha in FAOSTAT. All other fifteen sub-regional estimates had uncertainty bounds that contained the corresponding FAOSTAT values.

The uncertainty of CAM values was higher at regional compared to world level, i.e., up to 50% in Central Asia, South America and Southern Europe; up to 40% in Australia and New Zealand, South-eastern Asia and Southern Africa (Tab. 3). In absolute terms, South America had in addition the largest absolute uncertainty (80 Mha). Conversely, cropland area estimates with the smallest uncertainties (hence larger precision) were those for Southern Asia (13%), Northern America (20%), Northern Africa (24%), Eastern and Western Europe (25%).

Table 3. Regional cropland area estimates in CAM (means and uncertainties) and FAOSTAT. Melanesia, Micronesia, and Polynesia were excluded due to the cut-off country size used in this study.

Region	CAM	u	%u	FAO
	Mha	Mha	%	Mha
Eastern Africa	70	20	29%	78
Northern Africa	40	10	25%	50
Southern Africa	16	6	38%	14
Western Africa	60	20	33%	102
Middle Africa	16	7	44%	37

Northern America	200	40	20%	199
Central America and Caribbean	30	15	50%	37
South America	180	80	44%	131
Central Asia	40	20	50%	39
Eastern Asia	170	40	24%	145
Southern Asia	230	30	13%	240
South-eastern Asia	80	30	38%	123
Western Asia	50	10	20%	44
Eastern Europe	200	50	25%	197
Northern Europe	30	10	33%	19
Southern Europe	40	20	50%	37
Western Europe	40	10	25%	35
Australia and New Zealand	50	20	40%	32
World	1500	400	27%	1560

205

Figure 2. Regional comparisons between CAM and FAOSTAT data (R^2=0.92; NRMSE= 8%, p-value < 0.001). The dotted red line shows the perfect 1:1 relationship, while the black line shows the linear regression line of the points.
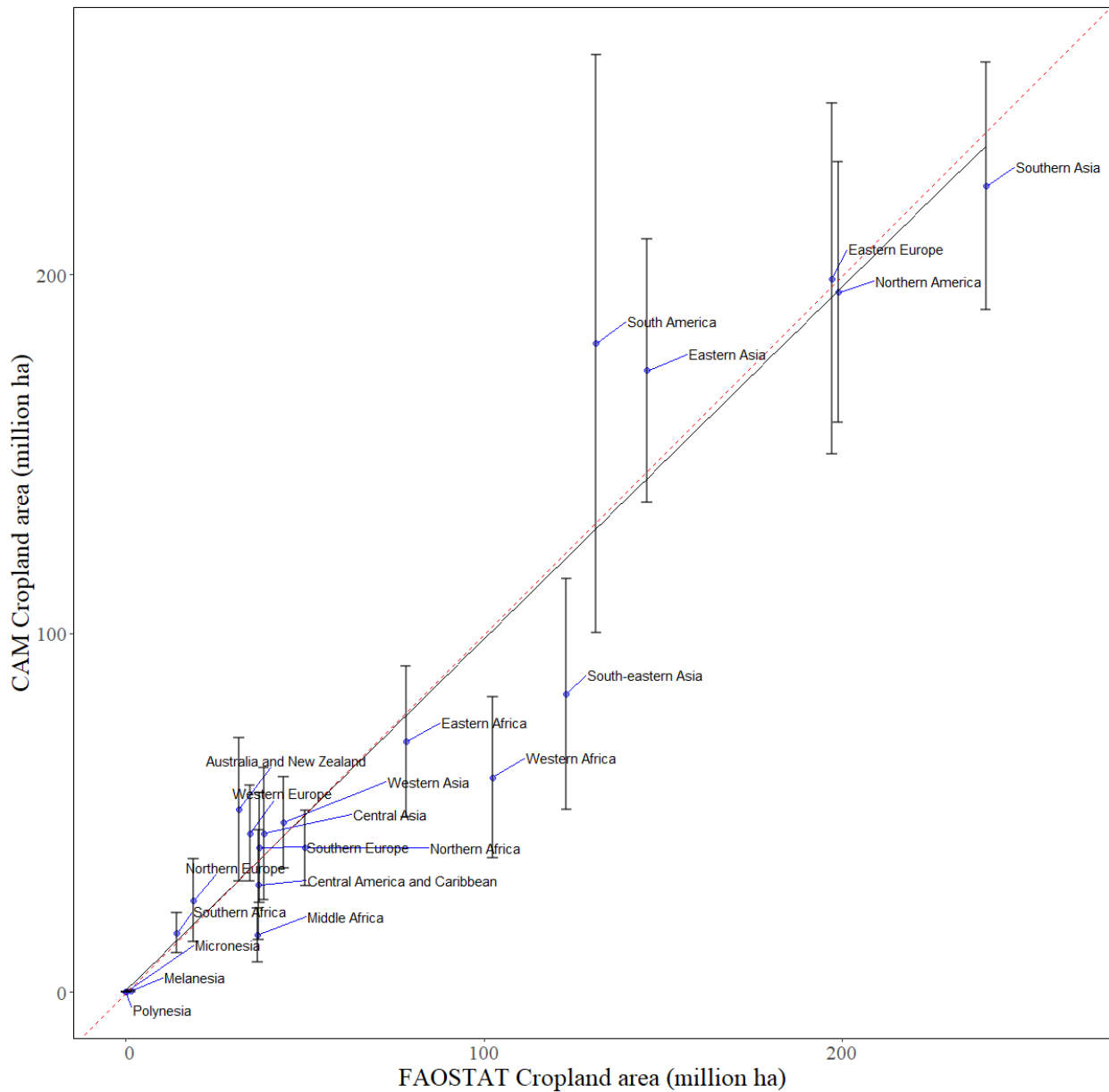
210

3.1.2 Country results

CAM estimates compared well with FAOSTAT statistics also at country level. Overall, considering the 182 countries and territories with cropland area greater than 10 kha, CAM values were in good agreement with FAOSTAT data (R^2 = 0.95; NRMSE of 3%, or less than 5 Mha on average). In addition, CAM estimates

215   were statistically consistent with FAOSTAT values for 114 of the 182 countries considered (Fig. 3).

Conversely, among CAM estimates that were inconsistent with FAOSTAT data, relevant cases (cropland area > 1 Mha) were Colombia (4 ± 3 vs. 9 Mha); Côte d'Ivoire (3 ± 2 vs. 8 Mha); the Democratic Republic of Congo (DRC) (5 ± 5 vs. 15 Mha); Indonesia (20 ± 10 vs. 59 Mha); Malaysia (3 ± 3 vs. 8 M ha); Niger (5 ± 4 vs. 18 Mha); Pakistan (21 ± 3 vs. 32 Mha); and the Philippines (6 ± 3 vs. 11 Mha). These highlight the need for further investigation of land cover maps and FAO statistics to better identify possible data quality issues.

Figure 3. Country comparisons between CAM and FAOSTAT (R^2=0.95; NRMSE= 3%, p-value < 0.001). The dotted red line shows the perfect 1:1 relationship, while the black line shows the linear regression line of the points.
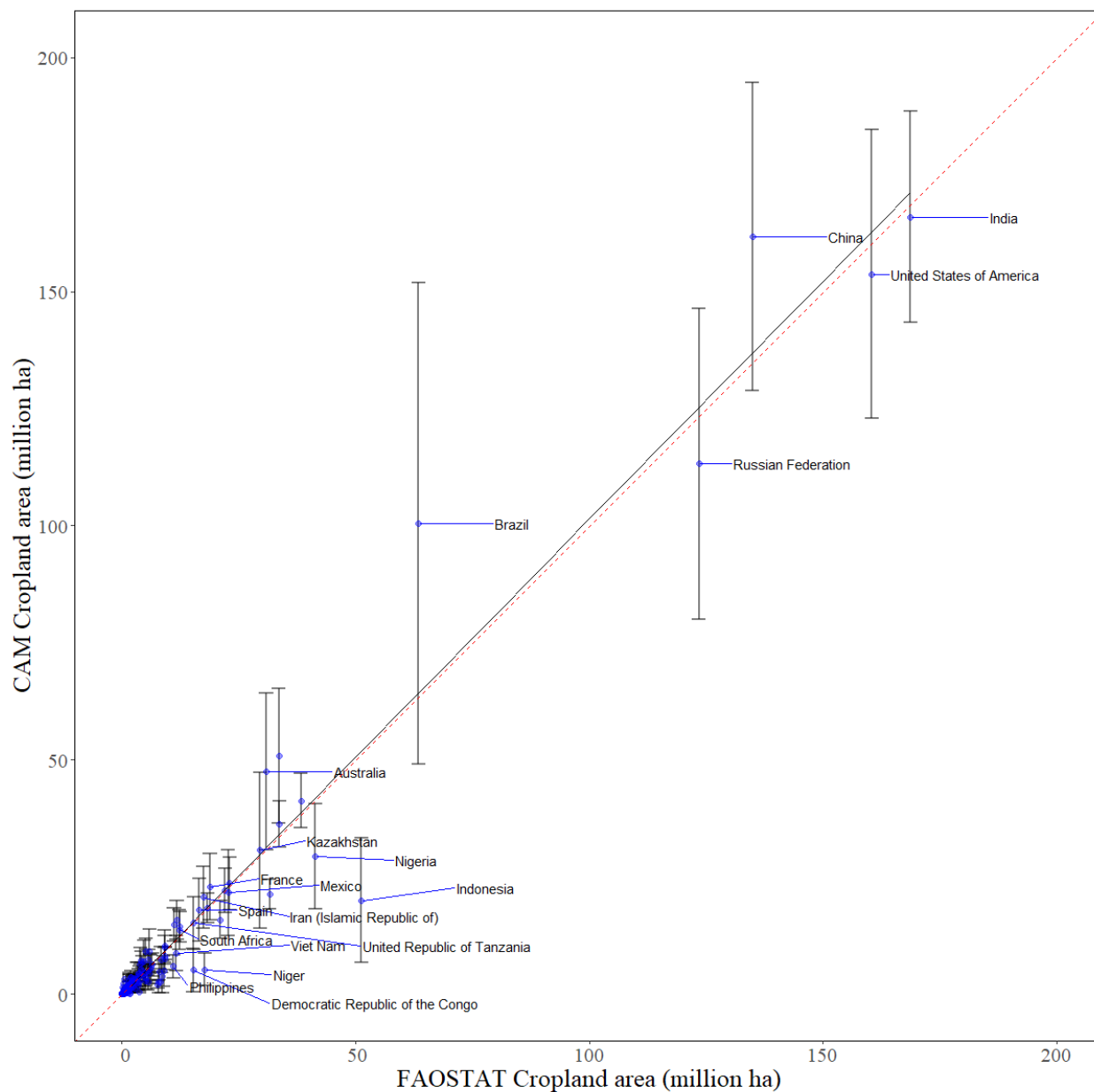
Overall, the large range of uncertainties found in the CAM aggregate country data, 20%–100%, underscored a large variability across geographies, in relation to: i) complexity of cropland landscapes; and/or ii) the ability of single land cover products to capture them consistently across regions. We note
230 nonetheless that among the top five countries in terms of cropland area extent (i.e., Brazil, USA, China, India, Russian Federation), only Brazil showed high uncertainty (50%) (Fig. 3). Countries with estimated cropland area greater than 1 Mha and relative uncertainties of 100% included Malaysia (3 Mha in absolute value), Nicaragua (2 Mha); Ireland (2 Mha); New Zealand (3 Mha); and DRC (5 Mha) (see also Appendix C).

235 **3.2 Simple cropland agreement**

3.2.1 Regional results

The CAM map and aggregation dataset complement the information on cropland area with knowledge of the contribution by agreement class. This information added useful insights into some of the findings highlighted above. First, the data show that the top agreement class, SA_6 was in general the larger
240 contributor to the estimated cropland area at regional level, with the exception of Africa (Fig. 4). This indicated that the underlying land cover maps were capable to map cropland rather consistently in most regions. More specifically, the sub-regions with the highest contribution of agreement class SA_6 (>50%) were: Northern America ($SA_6 > 62\%$), Eastern Europe ($SA_6 > 58\%$) Western Europe ($SA_6 > 56\%$) and Southern Asia ($SA_6 > 56\%$) (Appendix C, Tab. C1).

245 The large contribution of SA_6 was consistent with prevalence of simpler cropland landscapes in those regions —for instance, landscapes characterised by large fields with high-input and often irrigated annual crops. Conversely, the lowest contributions of SA_6 to cropland area were estimated in Middle Africa (2%), Western Africa (5%) and Eastern Africa (10%), followed by regions with shares of a quarter to a third, that is Central America (25%), Southern Africa (28%), Northern Africa (29%), Central Asia (32%), Australia
250 and New Zealand (33%). By the same reasoning as above, low shares of SA_6 were indicative of regions with prevalence of more complex agricultural mosaics—including in particular more traditional low-input systems. The latter characterize agriculture in Eastern, Middle and Western Africa regions. CAM aggregated data show that, unlike all other regions, in these three regions the SA_6 contribution to cropland area was in the single digits and far smaller than contributions from other agreement classes (Appendix C,
255 Tab. C1).

Figure 4. Percentage contribution to cropland area by simple cropland agreement, by subregion.
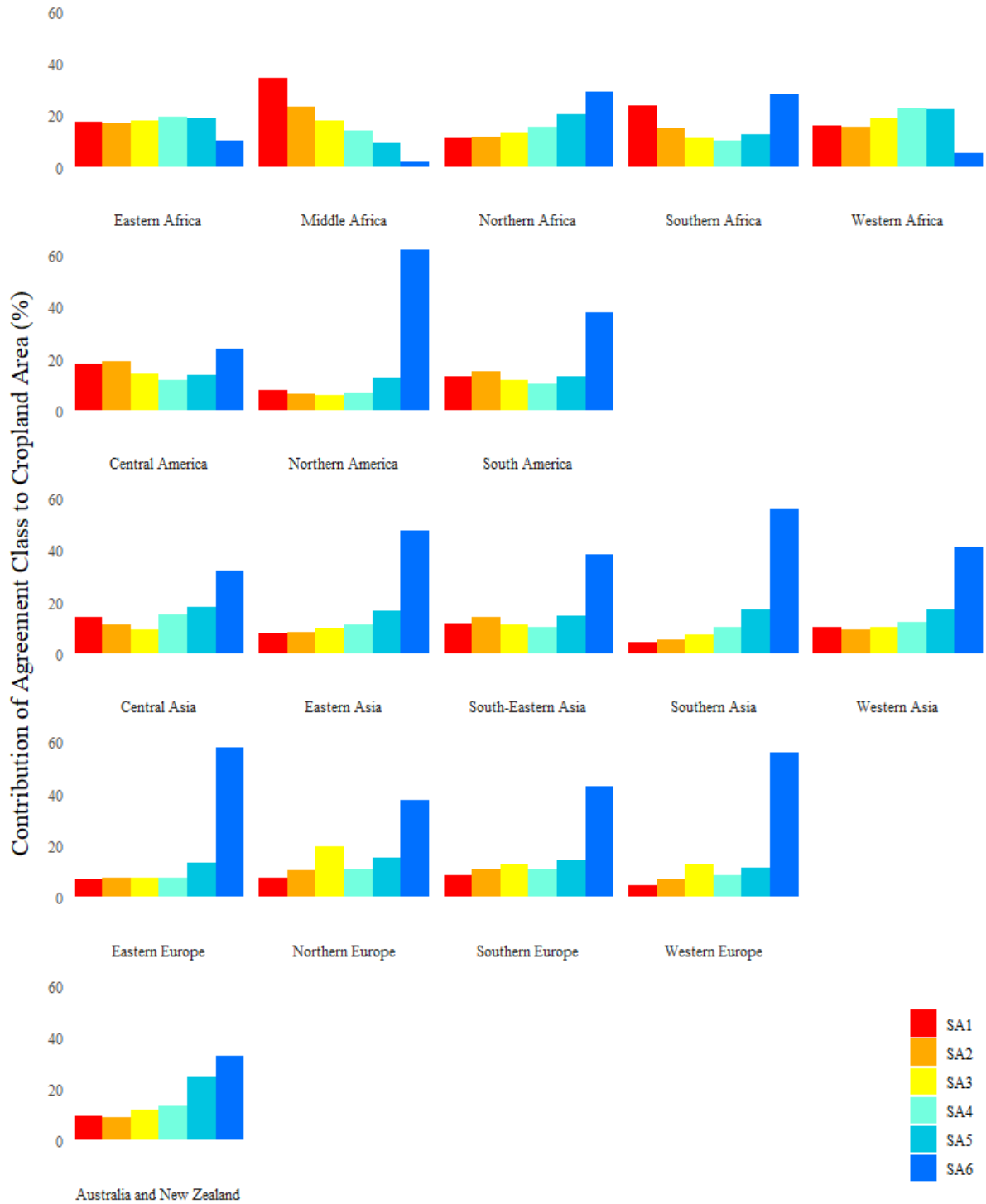
In terms of high SA_6 contributions to the regions identified above, it is likely that the underlying land cover products were mapping *temporary crops* or *arable land* at country level rather than cropland area, as also suggested by Tubiello et al. (2023b). These are in fact the specific sub-components of cropland included in all their definitions. Conversely, low SA_6 shares point to complex and fragmented agricultural landscapes in specific regions, where land cover products are likely to disagree. Indeed, we tested a possible relation between relative uncertainty in regional cropland area estimates and the level of contribution of top agreement classes (combined area of SA_4, SA_5 and SA_6) and found good correlation between the area uncertainty and the percent contribution to cropland area of the top three agreement classes (Fig. 5).

Figure 5. Linear regression of relative uncertainty in regional cropland area estimates against percent contribution to same cropland area by top-three agreement classes (R^2=0.46, NRMSE=64%, p-value<0.005).
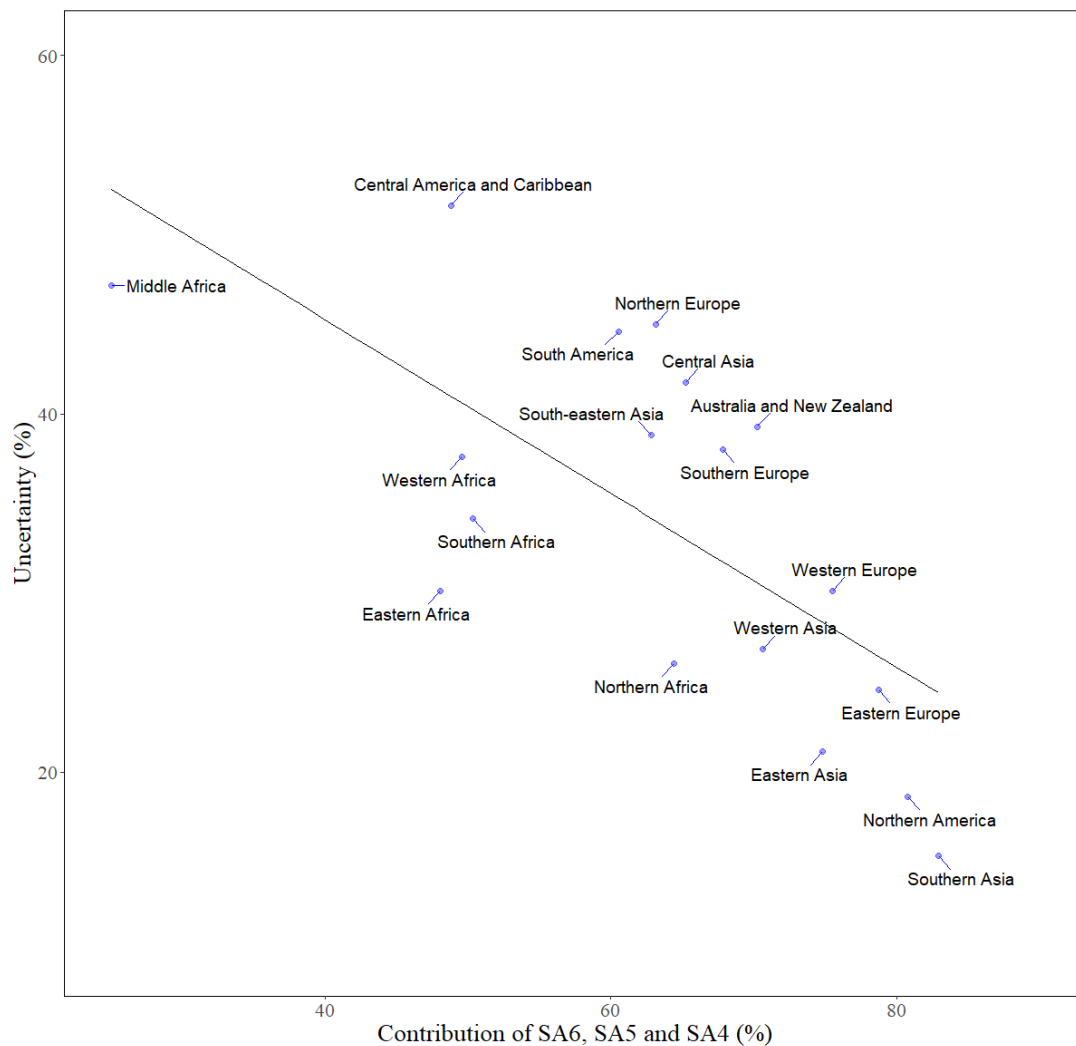
3.2.2 Country results

We extended the above analysis based on simple agreement classes to countries. The CAM country data confirmed the regional analysis of a strong link between simple cropland landscapes and prevalence of the SA_6 contribution to total cropland area. Only five countries globally had $SA_6 > 65\%$, of which four in Eastern Europe: Ukraine (75%), Bulgaria (70%), Hungary (70%), the Republic of Moldova (67%) and Canada (67 %). Cropland in these countries is indeed dominated by large, easy-to-recognize-from-space agricultural fields of annual crops (FAO, 2023a). In Ukraine, the top three agreement classes contributed 90% of the cropland area. Virtually the same features applied to other countries in Eastern and Central Europe, specifically Czechia (64%), Slovakia (64%), Romania (63%), Serbia (62%), Germany (62%) and Poland (61%); as well as in France and Austria, where it exceeded 50%.

Outside of Europe, Canada and the USA also had substantial proportions of SA_6 in their cropland areas, accounting for 67% and 61% respectively. In Central Asia, Turkmenistan and Uzbekistan show values comparable to Western European countries, with 52% and 57% respectively. In South-eastern Asia, large agreement in cropland classification is found in India (58%), Pakistan (63%), Bangladesh (56%), and Thailand (57%). Among African countries, Egypt stood out as the only one with a significant share from SA_6 (62%), likely due to the presence of the irrigated fields along the Nile and of pivot irrigation schemes against an otherwise arid landscape, which were well captured by the six classification algorithms.

Similarly and consistently with the regional findings, the CAM country data likewise suggested a relation between complexity of cropland landscapes and low SA_6 contribution. Indeed, of the 17 countries with SA_6 contribution below 10% and cropland size above 5 Mha (threshold chosen arbitrarily), 14 were located in Eastern, Middle or Western Africa, including Burkina Faso, Niger and DRC (0% SA_6 contribution, implying no agreement across the six maps in any pixel), Mozambique, Mali and Uganda (1%).

Finally, the highest uncertainties in estimated cropland area corresponded to high disagreement of the underlying land cover maps, expressed herein as the fraction covered by $SA_1 > 80\%$. These country cases included Papua New Guinea and Sierra Leone (SA_1=90%)(Appendix C, Tab. C2). The difficulties to map the fragmented and heterogeneous agricultural landscapes that prevail in these countries likely contributed to this feature (Potapov et al., 2022). In addition, in Papua New Guinea, cropland is dominated by permanent crops (FAO, 2023a), which most CAM input layers do not include in their definitions. This means that in such countries, CAM is mapping arable land rather than cropland.

Similar yet more complex dynamics were associated to country cases with 100% uncertainty in the CAM cropland estimates (Fig. 6). Two typologies could be identified among countries with cropland area > 1

Mha (Appendix C, Tab. C2). The first country case was characterized by high SA_1 percent contribution to
total cropland area, and included Nicaragua (50%), DRC (49%) and Malaysia (36%). As in the previous
cases, dominance of the SA_1 class was linked to complex landscapes within cropland, which could not be
mapped precisely, leading to high uncertainty. In particular, Malaysia was characterized by a large presence
of permanent crops, which was not mapped by all products. The second typology was characterized by high
SA_3 percent contributions to total cropland area and included Ireland (54%) and New Zealand (36%). In
both cases, despite little presence of permanent crops, disagreement across land cover products persisted.
We speculated that SA_3 prevalence was linked to the presence of crop/pasture mixtures within cropland, in
fact large shares of temporary meadows and pastures within arable land — a well-known landscape in both
countries — which are mapped only by a subset of the underlying land cover products, generating high
uncertainty as in the previous case, but for different reasons.

305

310

315 **Figure 6. Contribution to cropland area by cropland agreement class in 5 countries with 100%
uncertainty and cropland area > 1Mha.**
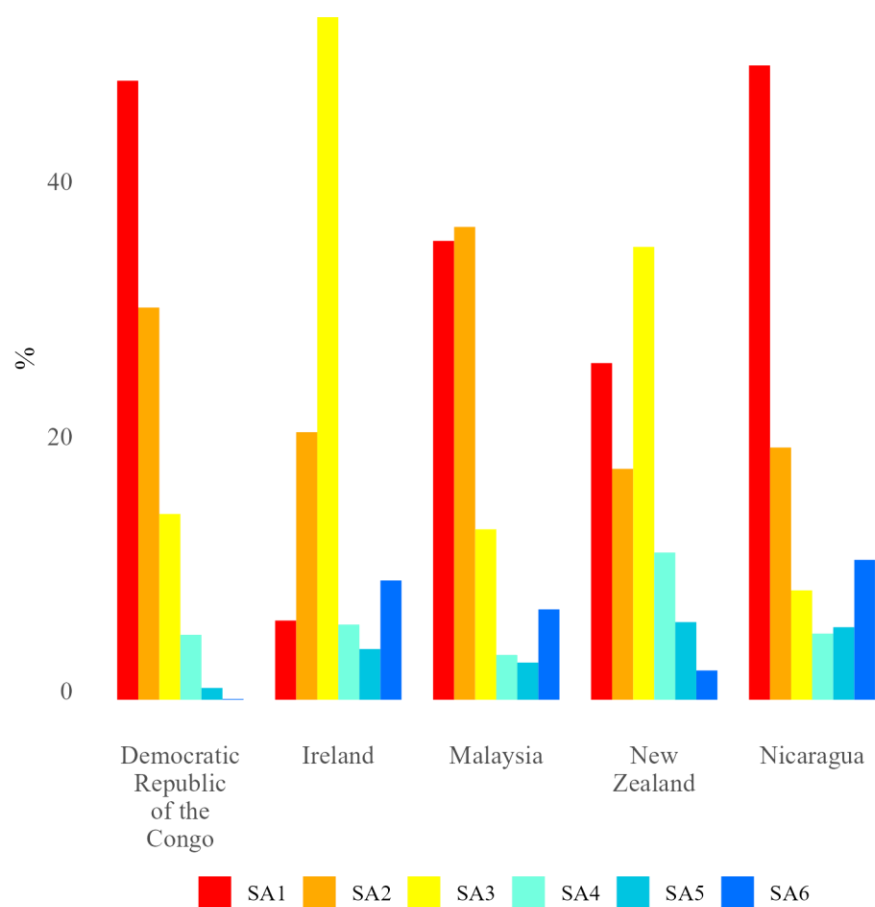
3.3 Detailed cropland agreement

3.3.1 Regional results

To gain further insight into the relationship between mapping uncertainty and landscape complexity, we looked at the detailed contribution of single CAM land cover maps to SA_1 contributions, by region, where SA_1 represents the areas with minimum agreement across land cover products. All detailed combinations at both regional and country levels are available in the CAM aggregation dataset (Tubiello et al., 2023a) but too large to be discussed herein in its entirety. We limited the discussion herein to the larger FAO regional groups and to notable country examples among those presented earlier.

Regionally and with reference to Fig. 7, GLAD contributed to SA_1 less than 1% in Europe to about 5% in Africa; WorldCover 1% in the Americas, Europe and Oceania to 9% in Africa; ESRI 4% in Europe to 11% in Oceania. Most contributions to SA_1 were instead from FCS30 (23% in Africa to 60% in Oceania); Globeland30 (23% in Oceania to 53% in Europe); and FROM_GLC (30% in Africa to 8% in Oceania).

Figure 7. Percent contribution to minimum cropland agreement area (SA_1), by input land cover product and region (ESR=ESRI; FCS30=GLC_FCS30-2020; FRG=FROM_GLC Plus; GLD=GLAD; GL30=Globeland30; WCO=WorldCover).
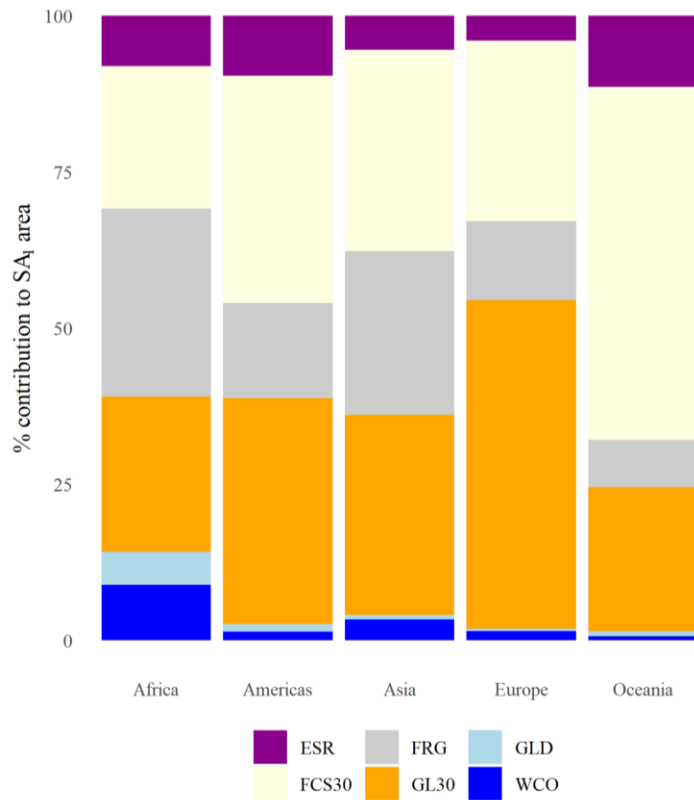
335 The regional analysis of the detailed agreement singles out FCS30 and Globeland30 as the land cover products in CAM map and dataset with the largest contribution to disagreement across regions, consistently with the fact that these are the only maps that include permanent crops, hence larger portions of cropland, in their definitions. Conversely ESRI, GLAD and WorldCover were the least contributors to disagreement, in line with their definitions, which focus on herbaceous crops within cropland landscapes. The

340 FROM_GLC was an intermediate case, consistently with its inclusion of shrub crops within its definitions.

3.3.2 Country results

In our earlier observations, we highlighted that Ireland and New Zealand had the largest contribution of SA_3, accounting for 54% and 36% respectively. This indicated that, on average, half of the land cover products in CAM agreed on mapping cropland. The detailed cropland agreement data in CAM showed that

345 in both countries, this outcome was due to a fixed combination of just three products: ESRI-FCS30-Globeland30 (Fig. 8). These were in fact the only land cover products in CAM that include pastures or generic herbaceous cover within their cropland definition, supporting our hypothesis that prevalence of SA_3 was linked to extensive areas of pastures within cropland, indeed typical of both countries' agricultural landscapes. Additionally, for New Zealand, the detailed agreement data indicated that FSC30 and FSC30-

350 GL30 were behind the SA_1 and SA_2 contributions to cropland area in the country. This was consistent with a significant presence of permanent crops in the national agricultural landscape, as both products were the only ones in CAM that could capture *permanent crops* within cropland area.

Figure 8. Percent contribution of products combinations to the detailed agreement, in Ireland and New Zealand. (Detailed agreement limited to land cover combinations with at least 3% contribution. ESR=ESRI;

355 FCS30=GLC_FCS30-2020; FRG=FROM_GLC Plus; GLD=GLAD; GL30=Globeland30; WCO=WorldCover).

For DRC, Malaysia, and Nicaragua (Fig. 9), countries characterized by cropland area estimates with very high uncertainty and a dominance of the SA_1 class, the information provided by the detailed agreement data

360 in CAM indicated that FCS30, GL30 and FRG were the land cover products mainly contributing to SA_1.

As discussed above, FCS30 and GL30 were the only two products in CAM that included permanent crops in their definitions. They compared in 8 out of 9 SA$_1$ combinations in DRC, 7 out of 8 in Malaysia, and in 5 out of 6 combinations in Nicaragua shown in Fig. 9, consistently with the large presence of *permanent crops* in these countries.

365   **Figure 9.** Percent contribution of products combinations to the detailed agreement, in the Democratic Republic of the Congo, Malaysia and Nicaragua. (Detailed agreement limited to land cover combinations with at least 3% contribution. ESR=ESRI; FCS30=GLC_FCS30-2020; FRG=FROM_GLC Plus; GLD=GLAD; GL30=Globeland30; WCO=WorldCover).
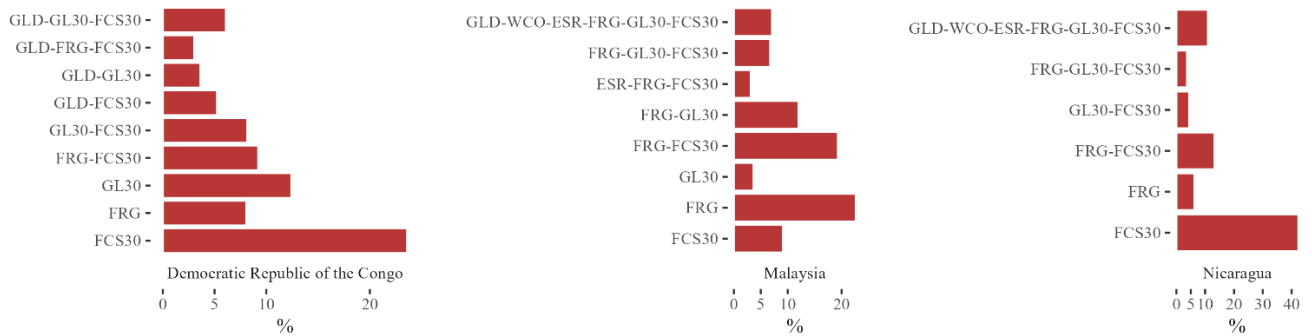
370

4. Data availability

The CAM aggregation dataset is publicly available in Zenodo at: https://doi.org/10.5281/zenodo.7987515 (Tubiello et al., 2023a).

5. Potential uses and limitations

375   The CAM aggregation dataset represents a novel global reference and knowledge product of the cropland area as well as a useful complement and guide for spatial applications of the CAM map (Tubiello et al., 2023b). For instance and unlike the underlying land cover maps applied in its synthesis the CAM dataset includes the uncertainty of cropland area estimates by country worldwide. By highlighting areas with lower consensus among the 6 cropland maps, it can thus guide and support the targeting of areas in need of more 380   in-depth spatial analysis. By the same token, thanks to the high spatial resolution and global coverage, pixels with higher agreement may support the development of global training datasets in machine learning approaches for future efforts of cropland mapping.

In constructing the CAM map and the CAM aggregate dataset we assumed that pixels and areas with higher agreement — corresponding in our approach to simple agreement classes SA$_4$ to SA$_6$ — have higher 385   likelihood to represent indeed cropland. The 6 cropland maps used in the construction of the CAM map differed by their operational definitions. Hence, we also assume that areas with larger consensus represent

cropland types and agricultural landscape that are common to the six cropland maps. The *temporary crops* (annual herbaceous crops) coincide with this core, common definitional component. Our tests (Appendix D, Fig. D1), provided statistical confirmation of this hypothesis although actual ground verification would be required for a conclusive assessment. The interpretation of pixels and areas with agreement classes SA_3 and below is instead less straightforward. A lower consensus may result from the errors of omissions and commissions that characterize each layer, their uneven accuracy across regions and in large countries but also to the differences in definitions or often a combination of all these elements. We acknowledge the fact that the 6 land cover layers suffer from inaccuracies across regions but maintain that our synthetic approach may help reducing the errors of input datasets. For instance, when comparing country statistics from each input layer and from CAM with FAOSTAT cropland areas, we observed the lowest NRMSE for the CAM aggregated dataset (Appendix D, Table D1). The detailed agreement data whereby we provided granular information on the agreement between each land cover product and their specific combinations can help to disentangle these more complex situations at multiple scales.

The CAM map and dataset currently provide information circa 2020. However, some of the maps used in our synthetic product (e.g. ESRI, GLAD and WorldCover, Globeland30) already include multi-year information and are expected to provide yearly land cover data on a regular basis. These future developments together with the addition of new cropland layers such as the WorldCereal of the European Space Agency (Van Tricht et al., 2023) when made operational on an annual basis may also provide opportunities for the analysis and understanding of cropland trends.

6. Conclusions

The CAM aggregation dataset presented herein consolidates information from six high-resolution global cropland maps circa 2020 currently available in the literature, using a meta-analysis approach to estimate cropland area and its uncertainty at country level, with data for 221 countries and territories and 34 regional aggregates. The CAM data are complemented by ancillary data on simple and detailed agreements of the underlying land cover products, with the same country and regional coverage. To our knowledge, this is the first time that such country information is presented in the literature.

The global regional and country examples provided in this work demonstrate the usefulness of the CAM aggregation dataset to assess current knowledge on cropland area in countries as available from land cover maps, highlighting how they agree or disagree on specific agricultural landscapes, depending on individual accuracy but also and importantly on definitional differences. In particular, the data highlighted critical connections between the level of complexity in the observed agricultural landscape and the preponderance

of specific cropland agreement classes. We showed that high agreement among land cover products corresponded to large scale fields with high input annual crops, hence cropland areas dominated by *temporary crops*; while minimum agreement tended to correspond to presence of more complex cropland landscapes, be it tree plantations in Africa, South-eastern Asia and South America, or mixed crop-pasture systems, such as in Ireland and New Zealand.

The CAM aggregation dataset represents a new global knowledge product and can serve as useful guide to support future land cover and land use product development and data evaluation.

7. References

Anghileri, D., Bozzini, V., Molnar, P., Jamali, A. A. J., and Sheffield, J.: Comparison of hydrological and vegetation remote sensing datasets as proxies for rainfed maize yield in Malawi, Agricultural Water Management, 262, 107375, https://doi.org/10.1016/j.agwat.2021.107375, 2022.

Bailey, J. T. and Boryan, C. G.: Remote sensing applications in agriculture at the USDA National Agricultural Statistics Service, Research and Development Division, USDA, NASS, Fairfax, VA, 2010.

Baroni-Urbani, C. and Buser, M. W.: Similarity of binary data, Systematic Zoology, 25, 251–259, https://doi.org/10.2307/2412493, 1976.

Bey, A., Sánchez-Paus Díaz, A., Maniatis, D., Marchi, G., Mollicone, D., Ricci, S., Bastin, J.-F., Moore, R., Federici, S., Rezende, M., and others: Collect earth: Land use and land cover assessment through augmented visual interpretation, Remote Sensing, 8, 807, https://doi.org/10.3390/rs8100807, 2016.

Bratic, G., Oxoli, D., and Brovelli, M.: Inter-Comparison of the Global Land Cover Maps in Africa Supplemented by Spatial Association of Errors, The International Archives of the Photogrammetry, Remote Sensing and Spatial Information Sciences, 42, 11–16, http://dx.doi.org/10.5194/isprs-archives-XLII-4-W14-11-2019, 2019.

Chaaban, F., El Khattabi, J., and Darwishe, H.: Accuracy assessment of ESA WorldCover 2020 and ESRI 2020 land cover maps for a Region in Syria, Journal of Geovisualization and Spatial Analysis, 6, 31, http://dx.doi.org/10.1007/s41651-022-00126-w, 2022.

Chen, J., Chen, J., Liao, A., Cao, X., Chen, L., Chen, X., He, C., Han, G., Peng, S., Lu, M., Zhang, W., Tong, X., and Mills, J.: Global land cover mapping at 30m resolution: A POK-based operational approach, ISPRS Journal of Photogrammetry and Remote Sensing, 103, 7–27, https://doi.org/10.1016/j.isprsjprs.2014.09.002, 2015.

Choi, S.-S., Cha, S.-H., and Tappert, C. C.: A survey of binary similarity and distance measures, Journal of systemics, cybernetics and informatics, 8, 43–48, 2010.

Defourny, P., Bontemps, S., Bellemans, N., Cara, C., Dedieu, G., Guzzonato, E., Hagolle, O., Inglada, J., Nicola, L., Rabaute, T., Savinaud, M., Udroiu, C., Valero, S., Bégué, A., Dejoux, J.-F., Harti, A. E., Ezzahar, J., Kussul, N., Labbassi, K., Lebourgeois, V., Miao, Z., Newby, T., Nyamugama, A., Salh, N., Shelestov, A., Simonneaux, V., Traore, P. S., Traore, S. S., and Koetz, B.: Near real-time agriculture monitoring at national scale at parcel resolution: Performance assessment of the Sen2-Agri automated system in various cropping systems around the world, Remote Sensing of Environment, 221, 551–568, https://doi.org/10.1016/j.rse.2018.11.007, 2019.

Ding, Y., Yang, X., Wang, Z., Fu, D., Li, H., Meng, D., Zeng, X., and Zhang, J.: A field-data-aided comparison of three 10 m land cover products in Southeast Asia, Remote Sensing, 14, 5053, https://doi.org/10.3390/rs14195053, 2022.

FAO: FAO GAUL: Global Administrative Unit Layers 2015, Country boundaries. In Earth Engine Data Catalog, https://developers.google.com/earth-engine/datasets/catalog (last access: 6 June 2023), 2015.

FAO: World programme for the census of agriculture 2020. Volume 2 Operational guidelines. FAO statistical development series 16. Rome. 348 pp. Licence: CC BY-NC-SA 3.0 IGO, FAO, Rome, 2018.

FAO: Land statistics. Global, regional and country trends, 1990-2018. FAOSTAT Analytical Brief Series No. 15. Rome, 2021.

FAO: FAOSTAT Land, Inputs and Sustainability: Land Use, https://www.fao.org/faostat/en/#data/RL, (last access: 6 June 2023), 2023a.

FAO: FAOSTAT Production: Crops and Livestock products, https://www.fao.org/faostat/en/#data/QCL, (last access: 6 June 2023), 2023b.

470 Fritz, S., See, L., You, L., Justice, C., Becker-Reshef, I., Bydekerke, L., Cumani, R., Defourny, P., Erb, K., Foley, J., and others: The need for improved maps of global cropland, Eos, Transactions American Geophysical Union, 94, 31–32, https://doi.org/10.1002/2013EO030006, 2013.

Gao, Y., Liu, L., Zhang, X., Chen, X., Mi, J., and Xie, S.: Consistency analysis and accuracy assessment of three global 30-m land-cover products over the European Union using the LUCAS dataset, Remote Sensing,
475 12, 3479, 2 https://doi.org/10.3390/rs12213479, 2020.

Gorelick, N., Hancher, M., Dixon, M., Ilyushchenko, S., Thau, D., and Moore, R.: Google Earth Engine: Planetary-scale geospatial analysis for everyone, Remote Sensing of Environment, https://doi.org/10.1016/j.rse.2017.06.031, 2017.

Graesser, J., Aide, T. M., Grau, H. R., and Ramankutty, N.: Cropland/pastureland dynamics and the
480 slowdown of deforestation in Latin America, Environmental Research Letters, 10, 034017, https://doi.org/10.1088/1748-9326/10/3/034017, 2015.

JCGM: JCGM 104:2009. Evaluation of measurement data — An introduction to the "Guide to the expression of uncertainty in measurement" and related documents, 2009.

Karra, K., Kontgis, C., Statman-Weil, Z., Mazzariello, J. C., Mathis, M., and Brumby, S. P.: Global land
485 use/land cover with Sentinel 2 and deep learning, in: 2021 IEEE international geoscience and remote sensing symposium IGARSS, 4704–4707, https://doi.org/10.1109/IGARSS47720.2021.9553499, 2021.

Karthikeyan, L., Chawla, I., and Mishra, A. K.: A review of remote sensing applications in agriculture for food security: Crop growth and yield, irrigation, and crop losses, Journal of Hydrology, 586, 124905, https://doi.org/10.1016/j.jhydrol.2020.124905, 2020.

490 Laso Bayas, J. C., Lesiv, M., Waldner, F., Schucknecht, A., Duerauer, M., See, L., Fritz, S., Fraisl, D., Moorthy, I., McCallum, I., Perger, C., Danylo, O., Defourny, P., Gallego, J., Gilliams, S., Akhtar, I. ul H., Baishya, S. J., Baruah, M., Bungnamei, K., Campos, A., Changkakati, T., Cipriani, A., Das, K., Das, K., Das, I., Davis, K. F., Hazarika, P., Johnson, B. A., Malek, Z., Molinari, M. E., Panging, K., Pawe, C. K., Pérez-Hoyos, A., Sahariah, P. K., Sahariah, D., Saikia, A., Saikia, M., Schlesinger, P., Seidacaru, E.,
495 Singha, K., and Wilson, J. W.: A global reference database of crowdsourced cropland data collected using the Geo-Wiki platform, Scientific Data, 4, 170136, https://doi.org/10.1038/sdata.2017.136, 2017.

Li, K. and Xu, E.: Cropland data fusion and correction using spatial analysis techniques and the Google Earth Engine, GIScience & Remote Sensing, 57, 1026–1045, https://doi.org/10.1080/15481603.2020.1841489, 2020.

500 Liu, L., Zhang, X., Gao, Y., Chen, X., Shuai, X., and Mi, J.: Finer-resolution mapping of global land cover: Recent developments, consistency analysis, and prospects, Journal of Remote Sensing, https://doi.org/10.34133/2021/5289697, 2021.

Liu, X., Yu, L., Li, W., Peng, D., Zhong, L., Li, L., Xin, Q., Lu, H., Yu, C., and Gong, P.: Comparison of country-level cropland areas between ESA-CCI land cover maps and FAOSTAT data, International Journal
505 of Remote Sensing, 39, 6631–6645, https://doi.org/10.1080/01431161.2018.1465613, 2018.

Lu, M., Wu, W., You, L., See, L., Fritz, S., Yu, Q., Wei, Y., Chen, D., Yang, P., and Xue, B.: A cultivated planet in 2010 – Part 1: The global synergy cropland map, Earth Syst. Sci. Data, 12, 1913–1928, https://doi.org/10.5194/essd-12-1913-2020, 2020.

Miller, D., McCarthy, J., and Zakzeski, A.: A fresh approach to agricultural statistics: data mining and
510 remote sensing, in: Proceedings of the Joint Statistical Meetings, August 1–6, 2009.

Monfreda, C., Ramankutty, N., and Foley, J. A.: Farming the planet: 2. Geographic distribution of crop areas, yields, physiological types, and net primary production in the year 2000, Global biogeochemical cycles, 22, https://doi.org/10.1029/2007GB002947, 2008.

Olofsson, P., Foody, G. M., Herold, M., Stehman, S. V., Woodcock, C. E., and Wulder, M. A.: Good practices for estimating area and assessing accuracy of land change, Remote sensing of Environment, 148, 42–57, https://doi.org/10.1016/j.rse.2014.02.015, 2014.

Pérez-Hoyos, A., Rembold, F., Kerdiles, H., and Gallego, J.: Comparison of global land cover datasets for cropland monitoring, Remote Sensing, 9, 1118, https://doi.org/10.3390/rs9111118, 2017.

Potapov, P., Turubanova, S., Hansen, M. C., Tyukavina, A., Zalles, V., Khan, A., Song, X.-P., Pickens, A., Shen, Q., and Cortez, J.: Global maps of cropland extent and change show accelerated cropland expansion in the twenty-first century, Nature Food, 3, 19–28, https://doi.org/10.1038/s43016-021-00429-z, 2022a.

Potapov, P., Hansen, M. C., Pickens, A., Hernandez-Serna, A., Tyukavina, A., Turubanova, S., Zalles, V., Li, X., Khan, A., Stolle, F., and others: The global 2000-2020 land cover and land use change dataset derived from the Landsat archive: first results, Frontiers in Remote Sensing, 3, 18, https://doi.org/10.3389/frsen.2022.856903, 2022b.

Saah, D., Johnson, G., Ashmall, B., Tondapu, G., Tenneson, K., Patterson, M., Poortinga, A., Markert, K., Quyen, N. H., Aung, K. S., Schlichting, L., Matin, M., Uddin, K., Aryal, R. R., Dilger, J., Ellenburg, W. L., Flores-Anderson, A. I., Wiell, D., Lindquist, E., Goldstein, J., Clinton, N., and Chishtie, F.: Collect Earth: An online tool for systematic reference data collection in land cover and use applications, Environmental Modelling & Software, 118, 166–171, https://doi.org/10.1016/j.envsoft.2019.05.004, 2019.

Stehman, S. V. and Foody, G. M.: Key issues in rigorous accuracy assessment of land cover products, Remote Sensing of Environment, 231, 111199, https://doi.org/10.1016/j.rse.2019.05.018, 2019.

Tang, F. H. M., Nguyen, T. H., Conchedda, G., Casse, L., Tubiello, F. N., and Maggi, F.: CROPGRIDS: A global geo-referenced dataset of 173 crops circa 2020, Earth System Science Data Discussions, 2023, 1–22, [preprint] https://doi.org/10.5194/essd-2023-130, 20 April 2023.

Tubiello, F. N., Conchedda, G., Casse, L., Pengyu, H., Chen, Z., De Santis, G., Fritz, S., and Muchoney, D.: High resolution cropland agreement map (30 m) circa 2020, [dataset] https://zenodo.org/record/7244124, 2022.

Tubiello, F. N., Conchedda, G., Casse, L., Pengyu, H., De Santis, G., and Zhongxin, C.: Cropland area database by country circa 2020, [dataset] https://doi.org/10.5281/zenodo.7987515, 2023a.

Tubiello, F. N., Conchedda, G., Casse, L., Pengyu, H., Zhongxin, C., De Santis, G., Fritz, S., and Muchoney, D.: Measuring the world's cropland area, Nature Food, 1–3, https://doi.org/10.1038/s43016-022-00667-9, 2023b.

Van Tricht, K., Degerickx, J., Gilliams, S., Zanaga, D., Battude, M., Grosu, A., Brombacher, J., Lesiv, M., Bayas, J. C. L., Karanam, S., Fritz, S., Becker-Reshef, I., Franch, B., Mollà-Bononad, B., Boogaard, H., Pratihast, A. K., and Szantoi, Z.: WorldCereal: a dynamic open-source system for global-scale, seasonal, and reproducible crop and irrigation mapping, Earth System Science Data Discussions, 2023, 1–36, [preprint] https://doi.org/10.5194/essd-2023-184, 2023.

Vancutsem, C., Marinho, E., Kayitakire, F., See, L., and Fritz, S.: Harmonizing and combining existing land cover/land use datasets for cropland area monitoring at the African continental scale, Remote Sensing, 5, 19–41, https://doi.org/10.3390/rs5010019, 2012.

Venter, Z. S., Barton, D. N., Chakraborty, T., Simensen, T., and Singh, G.: Global 10 m Land Use Land Cover Datasets: A Comparison of Dynamic World, World Cover and Esri Land Cover, Remote Sensing, 14, 4101, https://doi.org/10.3390/rs14164101, 2022.

555 Waldner, F., Schucknecht, A., Lesiv, M., Gallego, J., See, L., Pérez-Hoyos, A., d'Andrimont, R., Maet, T. de, Bayas, J. C. L., Fritz, S., Leo, O., Kerdiles, H., Díez, M., Tricht, K. V., Gilliams, S., Shelestov, A., Lavreniuk, M., Simões, M., Ferraz, R., Bellón, B., Bégué, A., Hazeu, G., Stonacek, V., Kolomaznik, J., Misurec, J., Verón, S. R., Abelleyra, D. de, Plotnikov, D., Mingyong, L., Singha, M., Patil, P., Zhang, M., and Defourny, P.: Conflation of expert and crowd reference data to validate global binary thematic maps, 560 Remote Sensing of Environment, 221, 235–246, https://doi.org/10.1016/j.rse.2018.10.039, 2019.

Wang, X., Gao, X., Zhang, Y., Fei, X., Chen, Z., Wang, J., Zhang, Y., Lu, X., and Zhao, H.: Land-cover classification of coastal wetlands using the RF algorithm for Worldview-2 and Landsat 8 images, Remote Sensing, 11, 1927, https://doi.org/10.3390/rs11161927, 2019.

Weiss, M., Jacob, F., and Duveiller, G.: Remote sensing for agricultural applications: A meta-review, 565 Remote sensing of environment, 236, 111402, https://doi.org/10.1016/j.rse.2019.111402, 2020.

Xu, Y., Yu, L., Feng, D., Peng, D., Li, C., Huang, X., Lu, H., and Gong, P.: Comparisons of three recent moderate resolution African land cover datasets: CGLS-LC100, ESA-S2-LC20, and FROM-GLC-Africa30, International Journal of Remote Sensing, 40, 6185–6202, https://doi.org/10.1080/01431161.2019.1587207, 2019.

570 Yu, L., Wang, J., Li, X., Li, C., Zhao, Y., and Gong, P.: A multi-resolution global land cover dataset through multisource data aggregation, Science China Earth Sciences, 57, 2317–2329, https://doi.org/10.1007/s11430-014-4919-z, 2014.

Yu, L., Du, Z., Dong, R., Zheng, J., Tu, Y., Chen, X., Hao, P., Zhong, B., Peng, D., Zhao, J., Li, X., Yang, J., Fu, H., Yang, G., and Gong, P.: FROM-GLC Plus: toward near real-time and multi-resolution land cover 575 mapping, GIScience & Remote Sensing, 59, 1026–1047, https://doi.org/10.1080/15481603.2022.2096184, 2022.

Zanaga, Daniele, Van De Kerchove, Ruben, De Keersmaecker, Wanda, Souverijns, Niels, Brockmann, Carsten, Quast, Ralf, Wevers, Jan, Grosu, Alex, Paccini, Audrey, Vergnaud, Sylvain, Cartus, Oliver, Santoro, Maurizio, Fritz, Steffen, Georgieva, Ivelina, Lesiv, Myroslava, Carter, Sarah, Herold, Martin, Li, 580 Linlin, Tsendbazar, Nandin-Erdene, Arino, Olivier. ESA WorldCover 10 m 2020 v100 (Version v100), https://doi.org/10.5281/zenodo.5571936, 2021.

Zhang, X., Liu, L., Chen, X., Gao, Y., Xie, S., and Mi, J.: GLC_FCS30: global land-cover product with fine classification system at 30\,m using time-series Landsat imagery, Earth System Science Data, 13, 585 2753–2776, https://doi.org/10.5194/essd-13-2753-2021, 2021.

Authors contribution

FNT GC and LC conceived the dataset and conducted the analysis. GC, LC, PH and ZC supported the underlying geospatial analysis. GD supported the land use analysis and country examples. All authors 590 contributed to writing the manuscript.

Competing interests

At least one of the (co-)authors is a member of the editorial board of Earth System Science Data.

Acknowledgements

The authors wish to acknowledge the Swiss Office of Agriculture for funding the FAO Statistics Division under the FAO Regular Programme, which made this work possible. The views expressed in this work are the authors' only and cannot be taken to represent FAO's views or policy on the subject matter.

595

8. Appendices

Appendix A. The six land cover products of the CAM maps and measures of spatial consistency and similarity

The six cropland layers that contribute to CAM include one thematic cropland product and five global land cover products, all containing one or multiple cropland classes (Tab. A1). GLAD, the thematic cropland map, uses images of multiple years (2016–2019) to create a single cropland map; a similar approach is used by FROM_GLC, Globeland30 (4 years) and the FCS30 (3 years) while ESRI and WorldCover use 2020 images. ESRI and Globeland30 make use of a combination of pixel- and object-based classification methods whereas the other products use pixel-based supervised classification approaches. Of the CAM components, WorldCover was openly available from the Earth Engine Data Catalog, while the other datasets were available through assets created by individual users in the GEE environment.

Table A1. Technical specifications of six land cover maps used as input in CAM maps (Tubiello et al., 2022; Tubiello et al., 2023b) and underlying information in the CAM aggregation dataset (Tubiello et al., 2023a).

Cropland layer	Spatial Resolution	Remote sensing data	Classification method	Algorithm	Source
ESRI	10m	Sentinel-2	Pixel & Object	Convolutional Neural Network	Karra et al., 2021
FROM_GLC Plus	30m	Landsat OLI & ETM+ MODIS	Pixel	Random Forest	Yu et al., 2022
GLAD	30m	Landsat Analysis Ready Data (ARD)	Pixel	Bagged Decision Tree Ensemble	Potapov et al., 2022a
GLC-FCS30-2020 (FCS30)	30m	Landsat, Sentinel-1SAR, SRTM DEM	Pixel	Local adaptive Random Forest	Zhang et al., 2021
GLOBELAND30	30m	Landsat TM5, ETM+ & OLI, HJ-1, GF-1	Pixel & Object (POK[a])	Pixel-Object-Knowledge Classifier	Chen et al., 2015
WORLDCOVER	10m	Sentinel-1 & 2, Copernicus Global DEM, RESOLVE Ecoregions 2017	Pixel & Position	Gradient Boosting Decision Tree Algorithm	Zanaga et al., 2021

[a]Pixel- and object-based methods with prior knowledge.

Spatial consistency and similarity of the six input layers in CAM were investigated following methods in Liu et al. (2021). A total of 30,000 random points among non-zero cropland values were selected, and cropland area fractions for each agreement layer separately, for all pixels within an area of 5 x 5 km around each random point. Areas of overlap were excluded from the analysis. This produced approximately 28,000 data points for each layer containing the location and cropland area fraction. Scatter plots were created where the cropland area fraction was plotted for each dataset pair. This allowed for a comprehensive analysis of the spatial similarity among datasets. The pixel-level comparison yielded the best agreement between the GLAD and the WorldCover (R^2 = 0.79; RMSE = 0.15), followed by WorldCover and ESRI (R^2 = 0.61, RMSE = 0.23), and ESRI and GLAD (R^2 = 0.58, RMSE = 0.24). On the contrary, lowest R^2 is found between FROM_GLC and the Globeland30 (R^2 = 0.26, RMSE = 0.36) and FROM_GLC and FCS30 (R^2 = 0.33, RMSE = 0.32) even though in absolute terms these products all mapped the largest global extents (Tab. A2). Overall, there is a clear separation between the three products that correlate well with one another (WorldCover, GLAD and ESRI) and the other high-resolution products. On the other hand, both Globeland30 and FCS30 have values that are almost consistently higher than in the GLAD. This suggests that there are many regions which are classified as cropland for Globeland30 and FCS30 where GLAD, but also WorldCover and ESRI, show no presence for cropland (Fig. A1 for pixel-comparison of the GLAD with the other six land cover maps).

Table A2. Pixel-level correlation (R^2) between the 6 cropland datasets, RMSE in brackets (values computed from fraction of the cropland area).

	ESRI	FROM_ GLC	GLAD	FCS30	Globeland30
FROM_GLC	0.4 (0.29)				
GLAD	0.58 (0.24)	0.5 (0.25)			
FCS30	0.45 (0.3)	0.33 (0.32)	0.48 (0.31)		
Globeland30	0.47 (0.32)	0.26 (0.36)	0.46 (0.33)	0.39 (0.27)	
WorldCover	0.61 (0.23)	0.53 (0.24)	0.79 (0.15)	0.49 (0.3)	0.47 (0.32)

Figure A1. Density scatterplot of correlation between GLAD and the other 5 cropland datasets. The colour of the points indicates the number of scatter points in that location. The black line depicts the regression line, while the red line shows the optimal 1:1 relationship.
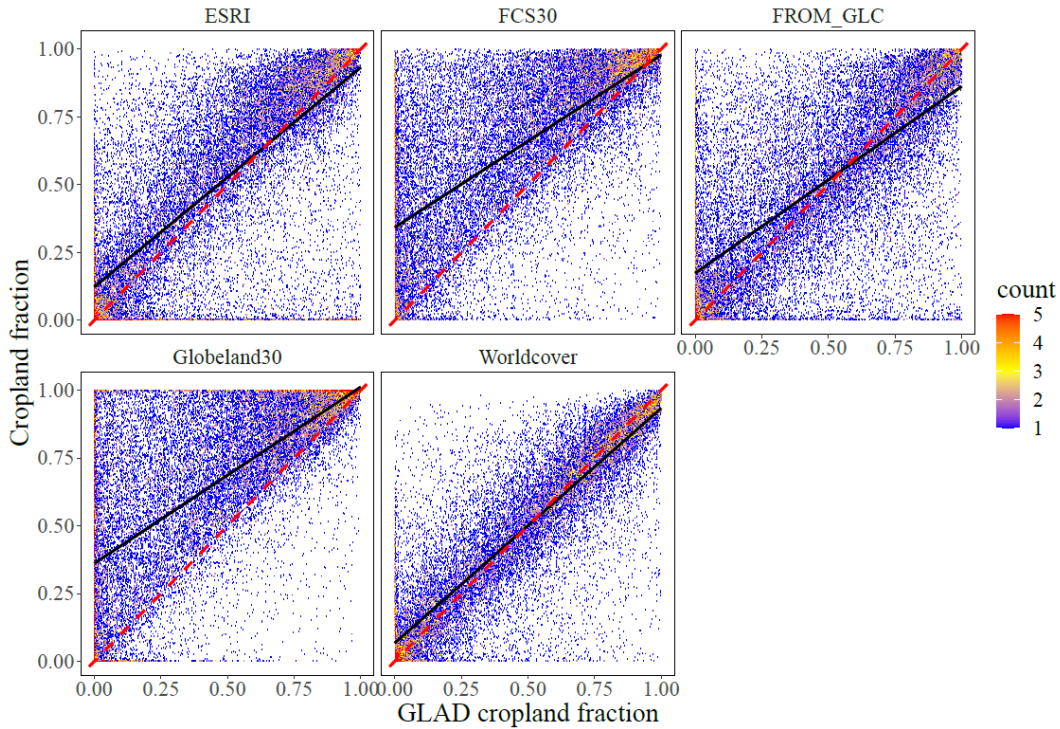
Binary similarity and distance measures are helpful tools in analysis of patterns and clustering (Choi et al., 2009). The detailed agreement allows to extract information on the binary instances between two cropland layers and to define for each country their intersections and their mismatches. We computed the Baroni similarity index (Baroni-Urbani and Buser, 1976) from country statistics of the detailed agreement. The Baroni similarity index ranges between 0 (no attributes in common between pairs of land cover products) and 1 (perfect overlap) and it thus accounts for both 'positive' – that is, where two layers agree on the presence of cropland—and 'negative' matches, corresponding herein to areas where two layers agree on the absence of cropland. The normalised index was computed as follows:

$$Similarity\ index_{ij} = \frac{\sqrt{AD} + A}{\sqrt{AD} + A + B + C} \tag{1}$$

Where i and j are cropland layers; A is the area that both layers mapped as cropland; B is area of cropland mapped by the first layer only; C is the area of cropland mapped by the second layer only; D is the country area that both layers agree is not cropland. In the analysis, the total A + B + C + D corresponds to the total land area (see Tab. A3 for regional and global results).

Table A3. Index of similarity, by region and globally.

	Africa	Americas	Asia	Europe	Oceania	World
ESRI_FROM_GLC	0.67	0.82	0.80	0.85	0.79	0.80
ESRI_GLB30	0.70	0.85	0.81	0.86	0.89	0.83
FCS30_ESRI	0.66	0.83	0.80	0.88	0.85	0.82
FCS30_FROM_GLC	0.75	0.78	0.82	0.82	0.73	0.80
FCS30_GLB30	0.75	0.84	0.82	0.87	0.88	0.83
GLB30_FROM_GLC	0.72	0.76	0.80	0.80	0.77	0.78
GLD_ESRI	0.72	0.89	0.86	0.89	0.89	0.86
GLD_FCS30	0.79	0.81	0.80	0.84	0.86	0.82
GLD_FROM_GLC	0.75	0.88	0.81	0.89	0.85	0.84
GLD_GLB30	0.81	0.82	0.81	0.81	0.89	0.82
GLD_WCO	0.83	0.92	0.89	0.93	0.92	0.90
WCO_ESRI	0.73	0.89	0.86	0.88	0.88	0.86
WCO_FCS30	0.76	0.82	0.82	0.84	0.81	0.82
WCO_FROM_GLC	0.75	0.86	0.81	0.87	0.87	0.83
WCO_GLB30	0.78	0.81	0.82	0.81	0.85	0.81
Average	0.74	0.84	0.82	0.86	0.85	0.83

Appendix B. Binary and decimal code attributes of the CAM detailed map of agreement

Table B1. Lookup table of the binary and decimal values for each detailed class of agreement. For each
685 datasets a value of 1 means presence of cropland and 0 is absence.

Value		Datasets					
Binary	Decimal	GLAD	WorldCover	ESRI	FROM_GLC	Globeland30	FCS30
000000	0	0	0	0	0	0	0
000001	1	0	0	0	0	0	1
000010	2	0	0	0	0	1	0
000011	3	0	0	0	0	1	1
000100	4	0	0	0	1	0	0
000101	5	0	0	0	1	0	1
000110	6	0	0	0	1	1	0
000111	7	0	0	0	1	1	1
001000	8	0	0	1	0	0	0
001001	9	0	0	1	0	0	1
001010	10	0	0	1	0	1	0
001011	11	0	0	1	0	1	1
001100	12	0	0	1	1	0	0
001101	13	0	0	1	1	0	1
001110	14	0	0	1	1	1	0
001111	15	0	0	1	1	1	1
010000	16	0	1	0	0	0	0
010001	17	0	1	0	0	0	1
010010	18	0	1	0	0	1	0
010011	19	0	1	0	0	1	1
010100	20	0	1	0	1	0	0
010101	21	0	1	0	1	0	1
010110	22	0	1	0	1	1	0
010111	23	0	1	0	1	1	1
011000	24	0	1	1	0	0	0
011001	25	0	1	1	0	0	1
011010	26	0	1	1	0	1	0
011011	27	0	1	1	0	1	1
011100	28	0	1	1	1	0	0
011101	29	0	1	1	1	0	1
011110	30	0	1	1	1	1	0
011111	31	0	1	1	1	1	1
100000	32	1	0	0	0	0	0
100001	33	1	0	0	0	0	1
100010	34	1	0	0	0	1	0

100011	35	1	0	0	0	1	1
100100	36	1	0	0	1	0	0
100101	37	1	0	0	1	0	1
100110	38	1	0	0	1	1	0
100111	39	1	0	0	1	1	1
101000	40	1	0	1	0	0	0
101001	41	1	0	1	0	0	1
101010	42	1	0	1	0	1	0
101011	43	1	0	1	0	1	1
101100	44	1	0	1	1	0	0
101101	45	1	0	1	1	0	1
101110	46	1	0	1	1	1	0
101111	47	1	0	1	1	1	1
110000	48	1	1	0	0	0	0
110001	49	1	1	0	0	0	1
110010	50	1	1	0	0	1	0
110011	51	1	1	0	0	1	1
110100	52	1	1	0	1	0	0
110101	53	1	1	0	1	0	1
110110	54	1	1	0	1	1	0
110111	55	1	1	0	1	1	1
111000	56	1	1	1	0	0	0
111001	57	1	1	1	0	0	1
111010	58	1	1	1	0	1	0
111011	59	1	1	1	0	1	1
111100	60	1	1	1	1	0	0
111101	61	1	1	1	1	0	1
111110	62	1	1	1	1	1	0
111111	63	1	1	1	1	1	1

Note: since we only have six datasets only 6 bits are shown for the binary value as the last 2 are always 0 (8-bit integer). An example: pixel value 38 equals bit 100110 meaning the 2nd, 3rd, and 6th bit (or datasets) depicts the presence of cropland (i.e. Globeland30, FROM_GLC and GLAD), whereas the other 3 layers show no cropland.

 Appendix C. CAM estimates for subregions and countries with largest relative uncertainty

Table C1. Percent area contribution by agreement class to regional cropland area estimates in CAM.

Region	SA$_6$	SA$_5$	SA$_4$	SA$_3$	SA$_2$	SA$_1$
Eastern Africa	10%	19%	19%	18%	17%	17%
Northern Africa	29%	20%	15%	13%	12%	11%
Southern Africa	28%	12%	10%	11%	15%	24%
Western Africa	5%	22%	23%	19%	16%	16%
Middle Africa	10%	19%	19%	18%	17%	17%
Northern America	62%	13%	6%	5%	6%	8%
Central America and Caribbean	25%	13%	11%	14%	19%	18%
South America	38%	13%	10%	12%	15%	13%
Central Asia	32%	18%	15%	9%	11%	14%
Eastern Asia	47%	16%	11%	9%	8%	8%
Southern Asia	56%	17%	10%	7%	6%	4%
South-eastern Asia	38%	14%	10%	11%	14%	12%
Western Asia	41%	17%	12%	10%	9%	10%
Eastern Europe	58%	13%	8%	7%	7%	7%
Northern Europe	38%	15%	11%	19%	10%	7%
Southern Europe	43%	14%	11%	13%	11%	8%
Western Europe	56%	11%	9%	13%	7%	5%
Australia and New Zealand	33%	24%	13%	12%	9%	9%

695 **Table C2**. Countries with 100% relative uncertainty in CAM estimates (mean area; SE; area by simple agreement class) and FAO cropland area.

Country	CAM	SE	SA1	SA2	SA3	SA4	SA5	SA6		FAO
	1000 ha									
Bahamas	50	50	42	7	1	0	0	0		12
Bhutan	50	50	25	12	6	3	2	1		100
Central African Republic	500	500	356	92	37	13	2	0		1880
Haiti	200	200	89	43	26	20	14	8		1350
Honduras	700	700	287	156	105	55	43	54		1596
Ireland	2000	2000	124	420	1071	118	80	187		445
Malaysia	3000	3000	1080	1113	401	105	88	213		8286
New Zealand	4000	4000	1057	725	1421	462	244	92		601
Nicaragua	2000	2000	995	396	172	104	114	220		1790
Panama	600	600	213	184	81	41	40	40		665
Papua New Guinea	300	300	253	33	9	4	1	0		1000
Timor-Leste	200	200	113	47	17	11	8	4		191
Puerto Rico	70	70	30	17	10	6	4	2		65
Qatar	20	20	7	3	3	2	2	2		24
Sierra Leone	200	200	181	16	3	1	0	0		1749
Western Sahara	10	10	8	2	0	0	0	0		4
Suriname	60	60	18	9	6	10	13	4		67
Eswatini	200	200	55	44	26	16	18	41		190
Trinidad and Tobago	20	20	10	5	3	1	1	0		47
United Arab Emirates	100	100	43	28	15	6	4	3		90
Democratic Republic of the Congo	5000	5000	2428	1538	729	255	46	3		15372
Montenegro	90	90	51	18	9	6	4	2		15

Appendix D. Comparison with FAOSTAT land use statistics

Figure D1. Scatterplots of the correlation between FAOSTAT land use statistics of Cropland and subcomponents (Arable land and Temporary crops) and the CAM area by aggregated classes of agreement. The black line depicts the regression line, while the red line shows the optimal 1:1 relationship. All correlations were statistically significant (p < 0.001).
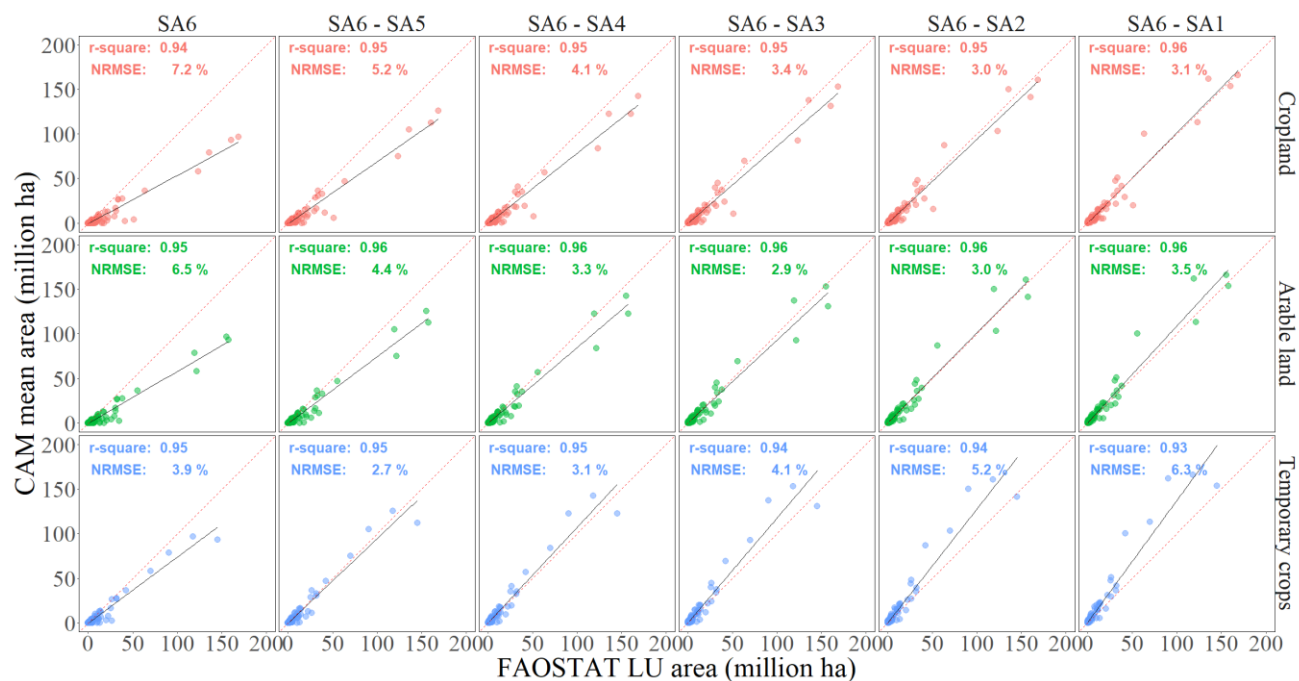
Table D1. Results of the comparison between country statistics from the 6 cropland input layers and from CAM with FAOSTAT cropland areas (R^2 and NRMSE).

Dataset	R^2	NRMSE (%)
ESRI	0.94	3.5
FCS30	0.89	6.5
FROM_GLC	0.94	3.4
GLAD	0.96	3.5
Globeland30	0.94	6.1
WorldCover	0.95	3.3
CAM	0.95	3.0